

A Manganese(II) Coordination Polymer Constructed from Phosphonate Ligand: Synthesis, Crystal Structure and Magnetic Properties^①

XU Yan^② LIU Bin LI Jie GAO Li

(Department of Materials Science and Engineering, Suqian College, Suqian 223800, China)

ABSTRACT A coordination polymer formulated as $[\text{Mn}(5\text{-pncH}_2)_2\text{H}_2\text{O}]$ (**1**, 5-pncH₃ = 5-phosphono-1-naphthalenecarboxylic acid), was hydrothermally synthesized and magnetically characterized. Compound **1** features a three-dimensional structure in which the inorganic chains of $[\text{Mn}(\text{O-P-O})]_n$ are cross-linked by the organic groups of phosphonate ligands. Magnetic measurements of **1** indicate that dominant antiferromagnetic interactions are mediated between the Mn^{II} centers.

Keywords: manganese, phosphonate ligand, crystal structure, magnetic properties;

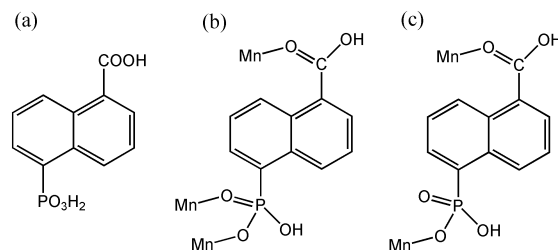
DOI: 10.14102/j.cnki.0254-5861.2011-2852

1 INTRODUCTION

The design and assembly of metal-organic complexes have been a current focus of interest because of their intriguing variety of architectures, fascinating topologies and promising applications in numerous areas, such as photochemistry, porosity, chemical sensing, magnetism, catalysis, and so forth^[1-10]. Phosphonate (RPO_3^{2-}) or phosphinate (RHPO_2^-) ligands can offer two or three oxygen donors to link the metal ions, as an important class of three-atom bridges, and have been used to construct a rich variety of complexes with unique network topologies^[11-15]. Metal phosphonates showing long range magnetic ordering have been reported, despite the fact that the exchange couplings mediated through the flexible O–P–O bridges can be weakly antiferromagnetic or even ferromagnetic^[16, 17], depending on the structural parameters such as the metal···metal distances and metal–O···O–metal torsion angles over the O–P–O

bridges. On the other hand, manganese-organic coordination polymers are well recognized from the magnetic point of view as the high-spin manganese(II) contains up to five unpaired electrons. Therefore, a considerable number of manganese(II)-carboxylate coordination polymers using a variety of carboxylates have been reported during the last decade^[18, 19]. However, compared to manganese(II)-carboxylate coordination polymers, few manganese(II)-phosphonate coordination polymers have been documented^[20].

In this paper, we report a novel manganese(II)-phosphonate coordination polymer using an 5-phosphono-1-naphthalenecarboxylic (5-pncH₃), namely, $[\text{Mn}(5\text{-pncH}_2)_2\text{H}_2\text{O}]$ (**1**). It shows a three-dimensional structure in which the inorganic chains of $[\text{Mn}(\text{O-P-O})]_n$ are cross-linked by the organic groups of phosphonate ligands. The magnetic measurements of **1** reveal that dominant antiferromagnetic interactions are mediated between the Mn^{II} centers.



Scheme 1. Molecular structure (a) and coordination mode (b,c) of 5-pncH₃

Received 20 April 2020; accepted 16 June 2020 (CCDC 1997696)

① This project was supported financially by Suqian Sci & Tech Program (No. K201911)

② Corresponding author. E-mail: xuyan0511@126.com

2 EXPERIMENTAL

2.1 Materials and physical measurements

All reagents and solvents were purchased from commercial sources and used without further purification. Elemental analyses (C, H and N) were performed on a Perkin-Elmer 240C elemental analyzer. IR spectra were recorded on a Bruker VERTEX70 spectrometer in the range of 400~4000 cm^{-1} using KBr pellets. Thermal analyses were performed using a PerkinElmer STA6000 TGA/DSC thermoanalyzer in a temperature range of 40~500 $^{\circ}\text{C}$ in N_2 flow (20 mL/min) at a heating rate of 10 $^{\circ}\text{C}/\text{min}$. Powder X-ray diffraction (XRD) data were collected on a Bruker D8 ADVANCE X-ray powder diffractometer with $\text{CuK}\alpha$ radiation ($\lambda = 1.54056 \text{ \AA}$) in a range of 5.00~50.00 $^{\circ}$ at room temperature.

2.2 Synthesis of $[\text{Mn}(\text{5-pncH}_2)_2\text{H}_2\text{O}]$ (**1**)

A mixture of $\text{Mn}(\text{CH}_3\text{COO})_2 \cdot 4\text{H}_2\text{O}$ (0.0491 g, 0.2 mmol) and 5-pncH₃ (0.0256g, 0.1 mmol) in 6 mL of water, adding 0.5 M NaOH solution 17 drops, was kept in a 10 mL Teflon-lined stainless container and heated at 140 $^{\circ}\text{C}$ for 48 h. The container was then cooled to room temperature. Brown rod-like crystals of compound **1** were obtained with 38.4% yield based on 5-pncH₃. Elemental analysis calcd. for $\text{C}_{22}\text{H}_{18}\text{MnO}_{11}\text{P}_2$: C, 45.93; H, 3.15%. Found (%): C, 46.23; H, 3.17 IR (KBr, cm^{-1}): 3321(m), 3099(w), 2906(w), 1688(s), 1612(w), 1512(m), 1428(w), 1284(m), 1210(w), 1164(w), 1072(s), 1056(s), 994(s), 972(s), 794(m), 610(m),

539(w), 505(w) cm^{-1} .

2.3 Structure determination

Single-crystal X-ray diffraction data were collected on a Bruker APEX-II CCD diffractometer using graphite-monochromated $\text{MoK}\alpha$ radiation ($\lambda = 0.71073 \text{ \AA}$) at 298 K. A hemisphere of data were collected in the θ range of 2.0~30.08 $^{\circ}$. The data were integrated using the Siemens SAINT program^[21], with the intensities corrected for Lorentz factor, polarization, air absorption, and absorption due to variation in the path length through the detector faceplate. Empirical absorption and extinction corrections were applied. The structures were solved by direct methods and refined on F^2 by full-matrix least-squares using SHELXTL^[22]. All the non-hydrogen atoms were refined anisotropically. All the hydrogen atoms except those attached to water molecules were put in calculated positions and refined isotropically with the isotropic vibration parameters related to the non-hydrogen atoms to which they are bonded. The hydrogen atoms attached to water molecules were found from Fourier maps and were refined isotropically.

Crystallographic data for **1**: $\text{C}_{22}\text{H}_{18}\text{MnO}_{11}\text{P}_2$, $M_r = 575.24$, monoclinic, Cc , $a = 10.0939(3)$, $b = 39.3493(12)$, $c = 6.9183(2) \text{ \AA}$, $\beta = 125.790(3)^\circ$; $V = 2228.97(13) \text{ \AA}^3$, $Z = 4$, $D_c = 1.714 \text{ g cm}^{-3}$, $\mu = 0.801 \text{ mm}^{-1}$, $F(000) = 1172$, $GOF = 1.017$, $(\Delta\rho)_{\text{max}} = 0.69$, $(\Delta\rho)_{\text{min}} = -0.23 \text{ e \AA}^{-3}$; final R indices ($I > 2\sigma(I)$) (R , wR): 0.0270, 0.0691, flack $x = -0.010(13)$. Selected bond lengths and bond angles are given in Table 1.

Table 1. Selected Bond Lengths (\AA) and Bond Angles ($^{\circ}$)

Bond	Dist.	Bond	Dist.	Bond	Dist.
Mn(1)–O(1)	2.169(3)	Mn(1)–O(4)	2.232(3)	Mn(1)–O(8)	2.188(3)
Mn(1)–O(3)	2.196(3)	Mn(1)–O(6)	2.188(3)	Mn(1)–O(1W)	2.168(3)
Angle	($^{\circ}$)	Angle	($^{\circ}$)	Angle	($^{\circ}$)
O(1)–Mn(1)–O(3A)	91.41(11)	O(6)–Mn(1)–O(3A)	93.29(11)	O(1W)–Mn(1)–O(1)	91.60(13)
O(1)–Mn(1)–O(4B)	88.63(11)	O(6)–Mn(1)–O(4B)	86.42(10)	O(1W)–Mn(1)–O(3A)	94.24(12)
O(1)–Mn(1)–O(6)	174.04(12)	O(8C)–Mn(1)–O(3A)	90.16(11)	O(1W)–Mn(1)–O(4B)	89.70(12)
O(1)–Mn(1)–O(8C)	88.90(11)	O(8C)–Mn(1)–O(4B)	85.90(11)	O(1W)–Mn(1)–O(6)	91.69(13)
O(3A)–Mn(1)–O(4B)	176.05(13)	O(8C)–Mn(1)–O(6)	87.43(12)	O(1W)–Mn(1)–O(8C)	175.56(12)

Symmetry transformation: A: $x, y + 1, z$; B: $-x, y, -z + 1/2$; C: $-x, -y + 1, -z$

3 RESULTS AND DISCUSSION

3.1 Infrared spectroscopy and powder

X-ray diffraction

The FTIR spectra of compound **1** are shown in Fig. 1a. The band at ca. 3321, 3099 cm^{-1} can be assigned to the stretching vibration of OH^- . The bands appearing at 1688, 1612 cm^{-1} correspond to the stretching vibration of COOH .

The absorption peaks 1072, 1056, 994 and 972 cm^{-1} correspond to the vibration of organic phosphonic acid group (CPO_3^{2-}). Powder X-ray diffraction (PXRD) pattern was studied at room temperature. The peak positions simulated by Mercury 3.3 and experimental PXRD patterns are in good agreement with each other, indicating the phase purity of compound **1** (Fig. 1b).

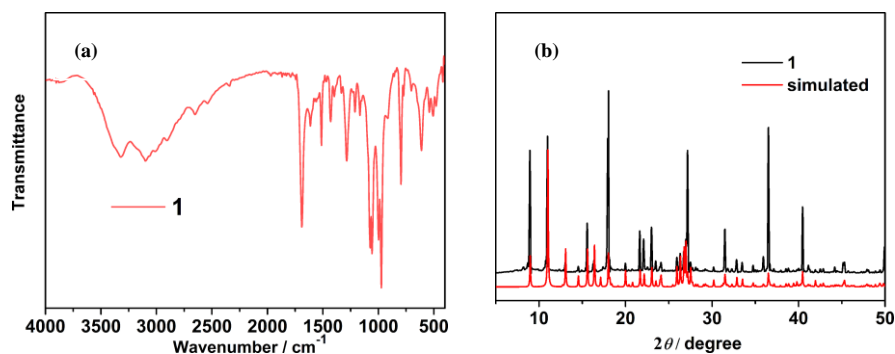


Fig. 1. IR spectra (a) and PXRD patterns (b) for compound **1**

3.2 Structural description

Single-crystal structural analysis reveals that **1** crystallizes in a polar space group Cc . The asymmetric unit consists of one Mn^{II} , two $5-pncH_2^-$, and one coordinated water molecule. The Mn(1) atom has a distorted octahedral coordination environment surrounded by three phosphonate oxygen atoms (O(3A), O(4B), O(8C)) (symmetry codes: A: $x, y + 1, z$; B:

$-x, y, -z + 1/2$; C: $-x, -y + 1, -z$), two carboxylate oxygen atoms (O(1), O(6)), and one water molecule (O(1W)) (Mn–O 2.168(3)~2.196(3) Å, the O–Mn–O bond angles lie in the range of 86.42(10)~176.05(13)°(Table 1)), as shown in Fig. 2a. The equivalent Mn atoms are bridged by O–P–O units forming a zigzag chain of $[Mn(O-P-O)]_n$ running along the c axis (Fig. 2b).

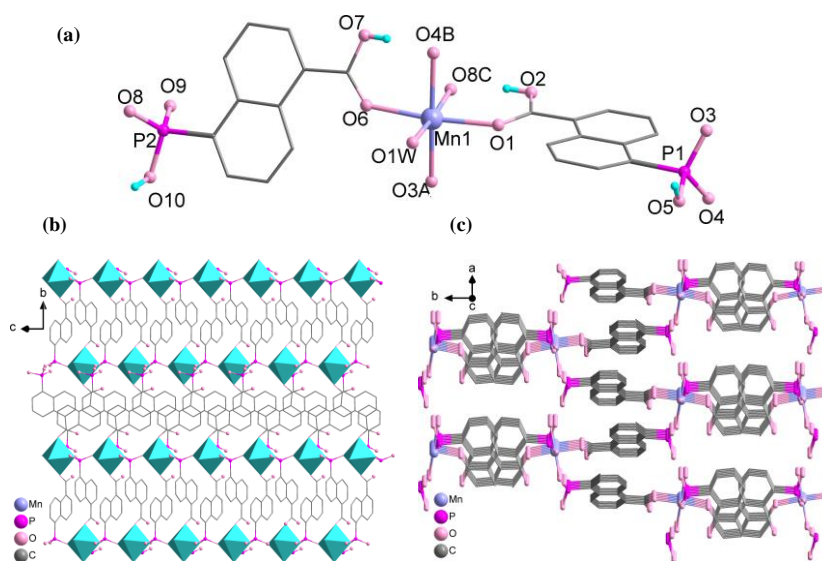


Fig. 2. (a) Building unit of **1** with atomic numbering scheme. Adjacent inorganic chains of $[Mn(O-P-O)]_n$ connected through phosphonate ligands in **1**. (c) Packing diagram of structure **1**

The coordination mode of $5-pncH_2^-$ in **1** is unique compared with those in the other metal carboxylate-phosphonates^[23, 24]. The $5-pncH_2^-$ acts as a tridentate ligand chelating and bridging three Mn atoms through two phosphonate oxygens, and one carboxylate oxygen (Scheme 1b and Fig. 2a). The remaining one phosphonate oxygen atom and one carboxylate oxygen are protonated. Another $5-pncH_2^-$ acts as a didentate ligand bridging two Mn atoms through one phosphonate oxygen, and one carboxylate oxygen (Scheme 1c and Fig. 2a). The remaining one

phosphonate oxygen atom and carboxylate oxygen are also protonated. The neighboring inorganic chains of $[Mn(O-P-O)]_n$ are connected to each other through phosphonate ligands, finally constructing a layer in the bc plane. 2D network structure is linked by phosphonate ligands into a 3D supramolecular network structure.

3.3 TGA analysis

The thermal stability of compound **1** was investigated under nitrogen atmosphere by thermogravimetric analysis (TGA). The result shows continuous loss above 230 °C.

Compound **1** loses one coordination water molecule (total weight loss: obs. 3.95%, calcd. 3.13%) in the 230~246 °C range, followed by the decomposition starting at 246 °C, in

which the organic components decomposed and the structure collapsed.

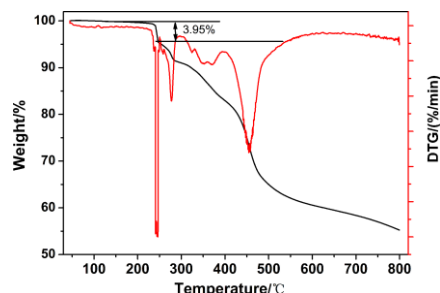


Fig. 3. TGA (black) and DTG (red) curves of compound **1**

3.4 Magnetic properties

The temperature dependent magnetic susceptibilities of **1** were measured in the temperature range of 2.0~300 K under an applied field of 1 kOe. Fig. 4 shows the $\chi_M T$ vs. T plot. The $\chi_M T$ value per Mn unit at 300 K is 4.12 $\text{cm}^3 \text{K mol}^{-1}$. This value is lower than the expected value for the spin-only value of 4.38 $\text{cm}^3 \text{K mol}^{-1}$ for one spin-only Mn^{2+} ion ($S = 5/2$, $g = 2$). Upon cooling, the $\chi_M T$ value

decreases continuously down to 2 K. The susceptibility data obey the Curie-Weiss law in the range of 2~300 K with a Curie constant of $C = 4.14 \text{ cm}^3 \text{K mol}^{-1}$ and a Weiss constant of $\theta = -7.92 \text{ K}$. The negative value of θ signifies antiferromagnetic interaction between the Mn^{II} ions bridged by O–P–O moiety^[25]. The magnetization $M(H)$ of compound **1** was also measured at 2 K, where no coercivity is observed.

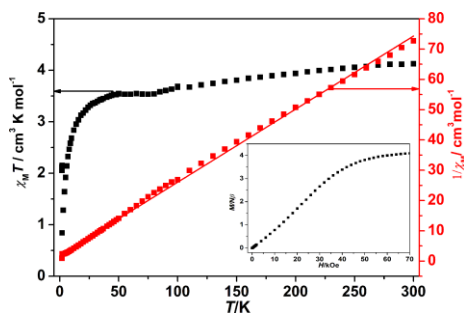


Fig. 4. Temperature dependence of $\chi_M T$ (■) and $1/\chi_M$ (■) for compound **1**. Inset: The magnetization curve measured at 2 K. Straight line shows the Curie-Weiss fitting

4 CONCLUSION

In summary, we report the novel manganese(II)-phosphonate compound based on a phosphonate ligand, namely, $[\text{Mn}(5\text{-pncH}_2)_2\text{H}_2\text{O}]$ (**1**). It exhibits a 3D structure in which O-P-O bridged neighbouring manganese(II), leading to an

inorganic chain $[\text{Mn}(\text{O-P-O})]_n$, further constructing a layer in the bc plane. 2D network structure is linked by phosphonate ligands into a 3D supramolecular network structure. Magnetic measurements of **1** indicate that dominant antiferromagnetic interactions are mediated between the Mn^{II} centers.

REFERENCES

- (1) Kurmoo, M. Magnetic metal-organic frameworks. *Chem. Soc. Rev.* **2009**, 38, 1353–1379.
- (2) Lee, J. Y.; Farha, O. K.; Roberts, J.; Scheidt, K. A.; Nguyen, S. T.; Hupp, J. T. Metal-organic framework materials as catalysts. *Chem. Soc. Rev.* **2009**, 38, 1450–1459.
- (3) Qin, L.; Hu, J. S.; Huang, L. F.; Li, Y. Z.; Guo, Z. J.; Zheng, H. G. Syntheses, characterizations, and properties of six metal-organic complexes based on flexible ligand 5-(4-pyridyl)-methoxyl isophthalic acid. *Cryst. Growth Des.* **2010**, 10, 4176–4183.
- (4) Du, J. J.; Yuan, Y. P.; Sun, J. X.; Peng, F. M.; Jiang, X.; Qiu, L. G.; Xie, A. J.; Shen, Y. H.; Zhu, J. F. New photocatalysts based on MIL-53

- metal-organic frameworks for the decolorization of methylene blue dye. *J. Hazard. Mater.* **2011**, 190, 945–951.
- (5) Wen, L. L.; Zhou, L.; Zhang, B. G.; Meng, X. G.; Qu, H.; Li, D. F. Multifunctional amino-decorated metal-organic frameworks: nonlinear-optic, ferroelectric, fluorescence sensing and photocatalytic properties. *Mater. Chem.* **2012**, 22, 22603–22609.
- (6) Meek, S. T.; Greathouse, J. A.; Allendorf, M. D. Metal-organic frameworks: a rapidly growing class of versatile nanoporous materials. *Adv. Mater.* **2011**, 23, 249–267.
- (7) Hu, Z. C.; Deibert, B. J.; Li, J. Luminescent metal-organic frameworks for chemical sensing and explosive detection. *Chem. Soc. Rev.* **2014**, 43, 5815–5840.
- (8) Zhang, W.; Xiong, R. G. Ferroelectric metal-organic frameworks. *Chem. Rev.* **2012**, 112, 1163–1195.
- (9) Yu, J. J.; Li, X. M.; Liu, B.; Zhou, S. A new Mn(II) complex assembled by 2,5-dihydroxy-1,4-benzenedicarboxylic acid and 2,2'-bipyridine: synthesis, structure and theoretical calculation. *Chin. J. Struct. Chem.* **2020**, 39, 765–771.
- (10) Li, Y.; Wu, J.; Gu, J. Z.; Qiu, W. D.; Feng, A. S. Temperature-dependent syntheses of two manganese(II) coordination compounds based on an ether-bridged tetracarboxylic acid. *Chin. J. Struct. Chem.* **2020**, 39, 727–736.
- (11) Liu, X. G.; Bao, S. S.; Huang, J.; Otsubo, K.; Feng, J. S.; Ren, M.; Hu, F. C.; Sun, Z.; Zheng, L. M.; Wei, S.; Kitagawa, H. Homochiral metal phosphonate nanotubes. *Chem. Commun.* **2015**, 51, 15141–15144.
- (12) Liu, M.; Feng, J. S.; Bao, S. S.; Zheng, L. M. Formation mechanism and reversible expansion and shrinkage of magnesium based homochiral metal-organic nanotubes. *Chem.-Eur. J.* **2017**, 23, 1086–1092.
- (13) Liu, X. G.; Zhou, K.; Dong, J.; Zhu, C. J.; Bao, S. S.; Zheng, L. M. Homochiral lanthanide phosphonates with brick-wall-shaped layer structures showing chiroptical and catalytic properties. *Inorg. Chem.* **2009**, 48, 1901–1905.
- (14) Liu, X. G.; Bao, S. S.; Zheng, L. M.; Li, Y. Z. Polymorphism in homochiral zinc phosphonates. *Inorg. Chem.* **2008**, 47, 5525–5527.
- (15) Huang, J.; Ding, H. M.; Xu, Y.; Zeng, D.; Zhu, H.; Zang, D. M.; Bao, S. S.; Ma, Y. Q.; Zheng, L. M. Chiral expression from molecular to macroscopic level via pH modulation in terbium coordination polymers. *Nat. Commun.* **2017**, 8, 2131–2142.
- (16) Liu, B.; Liu, J. C.; Shen, Y.; Feng, J. S.; Bao, S. S.; Zheng, L. M. Polymorphic layered copper phosphonates: exfoliation and proton conductivity studies. *Dalton Trans.* **2019**, 48, 6539–6545.
- (17) Jia, J. G.; Feng, J. S.; Huang, X. D.; Bao, S. S.; Zheng, L. M. Homochiral iron(II)-based metal-organic nanotubes: metamagnetism and selective nitric oxide adsorption in a confined channel. *Chem. Commun.* **2019**, 55, 2825–2828.
- (18) Tian, C. B.; He, Z. Z.; Li, Z. H.; Lin, P.; Du, S. W. Two new ferrimagnetic Mn(II)-carboxylate coordination polymers constructed from 5-tert-butyl isophthalic acid with (5/2, 15/2) and (5/2, 10/2) spin topologies. *CrystEngComm.* **2011**, 13, 3080–3086.
- (19) Escriche-Tur, L.; Font-Bardía, M.; Belén Albela, B.; Corbella, M. Determination of ZFS parameters from the EPR spectra of mono-, di- and trinuclear Mn(II) complexes: impact of magnetic coupling. *Dalton Trans.* **2017**, 46, 2699–2714.
- (20) Chandrasekhar, V.; Goura, J.; Sañudo, E. C. Carboxylate-free manganese(II) phosphonate assemblies: synthesis, structure, and magnetism. *Inorg. Chem.* **2012**, 51, 8479–8487.
- (21) *SAINT. Program for Data Extraction and Reduction.* Siemens Analytical X-ray Instruments, Madison, WI **1994–1996**.
- (22) *SHELXTL (Version 5.0), Reference Manual; Siemens Industrial Automation. Analytical Instruments:* Madison, WI **1995**.
- (23) Liu, B.; Liu, J. C.; Shen, Y.; Feng, J. S.; Bao, S. S.; Zheng, L. M. Polymorphic layered copper phosphonates: exfoliation and proton conductivity studies. *Dalton Trans.* **2019**, 48, 6539–6545.
- (24) Liu, B.; Xu, Y.; Bao, S. S.; Huang, X. D.; Liu, M.; Zheng, L. M. Enantioenriched cobalt phosphonate containing Δ -type chains and showing slow magnetization relaxation. *Inorg. Chem.* **2016**, 55, 9521–9523.
- (25) Pait, M.; Michael Shatruk, M.; Ray, D. Anion coordination selective [Mn₃] and [Mn₄] assemblies: synthesis, structural diversity, magnetic properties and catechol oxidase activity. *Dalton Trans.* **2015**, 44, 11741–11754.